Surface Barrier Resonances on a Simple Metal

S. Yang[a] and R. A. Bartynski[b]
Department of Physics and Astronomy and Laboratory for Surface Modification, Rutgers University, P.O. Box 849, Piscataway, New Jersey 08855-0849

G. P. Kochanski
AT&T Bell Laboratories, 600 Mountain Avenue, Murray Hill, New Jersey 07974

S. Papadia, T. Fondén, and M. Persson
Department of Applied Physics, Chalmers University of Technology, S-412 96 Göteborg, Sweden
(Received 2 November 1992)

We demonstrate the existence of a surface resonance below the vacuum level of a simple metal surface. Theoretical modeling of new scanning tunneling spectroscopy (STS) data from Al(111) shows that the mechanism for formation of this resonance is scattering from the bulk lattice. Correlation between the STS feature and structure seen in inverse photoemission (IPE) spectra from Al(111) suggests that the IPE feature is also attributed to this surface resonance, rather than a previously proposed matrix element effect.

PACS numbers: 73.20.At, 73.40.Gk

Image potential states at metal surfaces are formed when an electron with energy just below the vacuum level (E_{vac}) is trapped in a potential well bounded on the crystal side by a repulsive barrier associated with a bulk band gap and on the vacuum side by the imagelike part of the surface barrier. The inverse dependence on distance from the surface of the image potential leads to a Rydberg-like series of states that converge to the continuum at E_{vac}. These states have been of experimental and theoretical interest for several years [1–4] due to in part the constraints they place on the shape of the surface potential barrier extending into the vacuum.

The image potential has a significant effect on charge exchange and neutralization in ion-surface scattering and desorption [5], vacuum tunneling phenomena [6–9], and low energy electron diffraction (LEED) [1, 10]. In addition, the surface barrier region is complex theoretically, as the local density approximation is no longer valid and the long-range part of the electron-electron correlations dominates [11].

In contrast to the experimental work, the theoretical description of these phenomena usually employs free-electron-like metal surfaces, such as Al(111), which have no projected band gaps. However, the surface electronic structure near the vacuum level of such systems remains controversial. The only published inverse photoemission (IPE) spectrum from clean Al(111) [12] revealed a spectral feature ~ 0.5 eV below E_{vac}. This feature was interpreted as an image potential resonance, but without a band gap, the origin of the electron reflectivity on the crystal side of the surface barrier was unclear. Exploring this issue, Lindgren and Walldén [3] found a well defined peak in the density of states (DOS) of a jellium surface bounded by a truncated image potential, but when this truncation was replaced by a more realistic approximation of the surface potential, the DOS had no structure below E_{vac}. Subsequently, Papadia, Persson, and Salmi [4] found that even far away from a band gap, the modulation of the crystal potential due to the Al ion cores gives rise to sufficient reflectivity for such a resonance to appear in the surface DOS. The DOS interpretation of the IPE spectral feature was recently challenged by Schaich and Lee [13] who claimed that this feature may simply be an artifact of the inverse photoemission technique. In calculating the response of a jellium surface, they found that the matrix element governing IPE obtained an oscillatory component leading to a series of peaks in the isochromat photon yield as the final state electron energy approached E_{vac} from below. Such results have potentially serious implications on the interpretation of both photoemission and inverse photoemission data in general, and spectral features associated with surface resonances in particular.

In this Letter, we present new inverse photoemission and scanning tunneling spectroscopy data from the Al(111) surface that demonstrate the existence of a resonance in the surface DOS below E_{vac} where no bulk band gap exists. The image potential feature observed in **k**-resolved inverse photoemission (KRIPE) spectra is correlated with a peak observed below E_{vac} in scanning tunneling spectroscopy (STS) data. Theoretical modeling of the electronic structure and the tunneling spectra of a jellium surface where the crystal potential is included perturbatively show that this feature derives from a crystal-induced image resonance in the surface DOS of the Al crystal. The fact that two such divergent techniques that depend on very different couplings to the surface electronic structure yield similar results strongly

© 1993 The American Physical Society

supports an interpretation in terms of the surface density of states in contrast to matrix element effects only.

The IPE and STS data were obtained from the same Al(111) crystal which was oriented with Laue x-ray back diffraction to within 0.3° of the ⟨111⟩ axis. Prior to insertion into the vacuum chamber, the surface was chemically etched. In the chamber, an atomically clean surface was prepared by repeated cycles of Ne^+ ion bombardment and thermal annealing to 410 °C. This resulted in a surface that Auger electron spectroscopy showed was free from contamination and exhibited a sharp LEED pattern. Inverse photoemission data were obtained using an isochromat spectrometer described in detail elsewhere [14]. A highly collimated ($\delta\theta \sim 3°$), monoenergetic beam of electrons, swept through the range of 4–16 eV, impinged on the Al(111) sample while photons emitted at an energy of 9.5 eV were detected by a Geiger-Müller tube filled with iodine vapor and terminated with a SrF_2 window. The overall energy resolution was ~ 0.4 eV. The STS measurements were performed on a UHV scanning tunneling microscope (STM) with an iridium tip that is described in an earlier publication [15]. Topographic images of the surface showed average terrace widths of ~ 100 Å and all spectroscopic measurements were taken near the center of a terrace. We measure the differential conductance $\frac{dI}{dV}$ at constant average tunneling current [6], to allow a wider range of voltages than would be possible with a measurement at constant height.

The tunneling data have been interpreted using the quasi-one-dimensional model calculation first developed for the interpretation of inverse photoemission data [4] and now extended to the calculation of conductance curves versus bias voltage [16]. The tip and sample are modeled separately by a semi-infinite jellium with an electron-gas-density parameter, $r_s = 2.07$, appropriate for Al. Uniform external fields F and $-F$ are applied on the tip and substrate jellium, respectively, accounting for different bias voltages and tip-surface separations. The external fields are incorporated self-consistently for each part as in Ref. [17] and matched together in their asymptotic linear region. In order to obtain the long-range, image potential of the metal surface, we proceed as proposed by Serena, Soler, and Garcia [18] when calculating the exchange-correlation potential. This scheme uses the local density approximation (LDA) in the bulk and up to the image-plane location, and beyond that, a nonlocal form of the potential. This approach ignores exchange effects on the location of the image plane that start to be important first at larger r_s as shown in Ref. [11].

The scattering of the electrons from the Al ion cores is treated by the Born approximation in the weak crystal pseudopotential in the same manner as described in Ref. [4]. This approximation is well justified for energies far from a bulk band gap [16]. In our case for energies around E_{vac} the closest band gap is ~ 6 eV away [19]. In this model we obtain a crystal reflectivity $r_C \sim 0.1$ that is taken into account when we integrate the one-electron Schrödinger equation in the tip-substrate potential. The tunnel current is then found from the transmission coefficient of the normalized wave function across the barrier. We have assumed that the tunneling occurs from the Fermi level only. The resulting conductance curves, $\frac{dI}{dV}$, are taken under the condition of constant average tunnel current, which implies that F has to be altered for each bias V.

Typical inverse photoemission spectra obtained from the Al(111) surface are presented in Fig. 1. The distinct peak at 3.75 eV above E_F in the normal incidence spectrum is the image potential related feature addressed in this paper that previously only was observed at normal incidence [12]. As can be seen, the image feature disperses to higher energy, broadens, and diminishes in intensity with increasing angle of incidence. The inset in Fig. 1 shows that the parabolic free electron dispersion that best fits the observed dispersion of the image feature with parallel momentum $\mathbf{k}_\parallel$ has an effective mass of $\frac{m^*}{m} = 1.08 \pm 0.1$. These observations alone cannot dis-

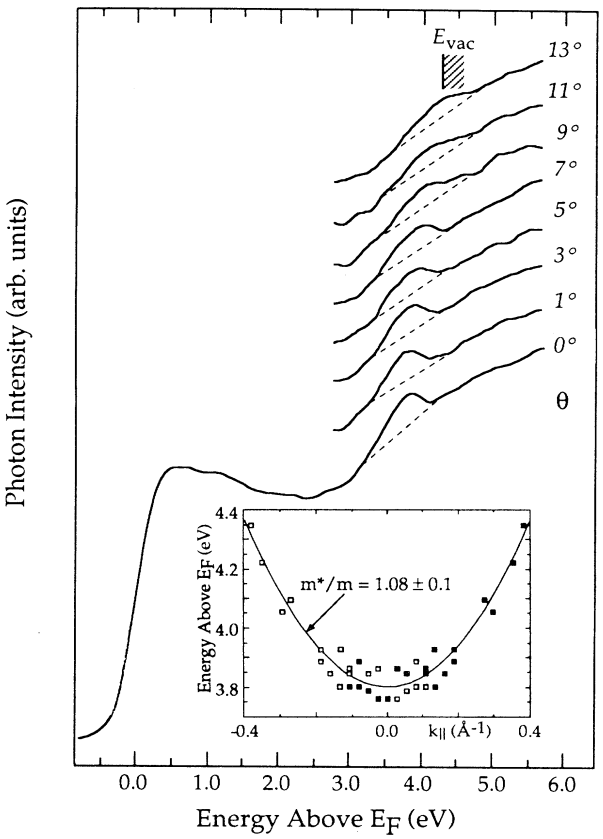

FIG. 1. Inverse photoemission spectra from the Al(111) surface obtained in the isochromat mode at a photon energy of 9.5 eV. Off-normal spectra are shifted vertically for clarity. Inset: Dispersion of the image potential induced feature with momentum parallel to the surface. The solid curve is a parabolic fit to the dispersion.

tinguish between the two interpretations of this feature since a value of effective mass close to unity is expected for either a matrix element effect [13] or a true resonance.

An alternative way to probe the density of states at a metal surface that avoids possible complications of the inverse photoemission matrix element is tunneling spectroscopy. If a resonance is present on the Al(111) surface, the differential conductance should increase on resonance and decrease away from resonance, creating an oscillatory component to the $\frac{dI}{dV}$ curves, thus reflecting the DOS [6, 7, 20]. If, on the other hand, the KRIPES feature is a matrix element effect, then no such oscillation is expected below E_{vac} in the tunneling data.

In order to examine the effect of the crystal potential on the $\frac{dI}{dV}$ curves in detail, we first calculate the induced phase shift derivative with respect to energy, $\frac{\partial\Phi}{\partial\epsilon}$, which is directly proportional to the induced density of states $n(\epsilon)$ [21]. The results for $\frac{\partial\Phi}{\partial\epsilon}$ for a jellium surface with and without the crystal potential and in the presence of an external field are shown in Fig. 2(a). We find in both situations an oscillatory structure in $\frac{\partial\Phi}{\partial\epsilon}$ where both the amplitude and the number of oscillations increases when the crystal potential is included. The oscillations at energies above E_{vac} are analogous to the Gundlach resonances [22] and are due to reflection back and forth of the electron wave between the repulsive field induced linear part of the potential and the sharp potential transition when going from the surface to the bulk. The most important feature is the presence of a peak below the metal vacuum level for any finite value of the external field, but only when the crystal potential is included. This peak is simply a field-shifted version of the crystal-induced resonance identified in Ref. [4]. Comparing the $\frac{\partial\Phi}{\partial\epsilon}$ curves of Fig. 2(a) with the $\frac{dI}{dV}$ curves in Fig. 2(b), we see a clear one-to-one correspondence between the respective resonances and peaks. The crystal-induced resonance in the surface DOS is clearly identified in $\frac{dI}{dV}$ since it disappears when the crystal potential is removed.

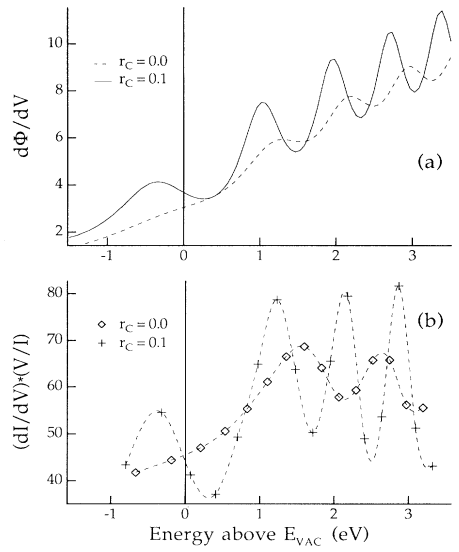

FIG. 2. (a) Calculated energy derivative of the induced phase shift, proportional to $n(\epsilon)$, for an external field value of 0.20 eV/Å. Here, the field strength is constant for all energies. r_C is the crystal reflectivity assumed in the calculation (see text). In the dashed curve, the contribution from the crystal reflectivity is ignored. The solid curve includes scattering from the Al lattice that results in a new peak below the metal vacuum level. A surface resonance occurs below E_{vac} only if the crystal potential is included. (b) Calculated differential conductance ($\frac{dI}{dV}$) curves with (+) and without (diamond) inclusion of the crystal potential. The initial field strength F is also 0.20 eV/Å here, but applies only to the first points. To satisfy the requirement of constant tunnel current throughout the calculations, the field strength was changed with increasing bias, V. The dashed lines between the points are cubic spline interpolations and serve primarily as a guide to the eye. A spectroscopic feature below E_{vac} associated with a resonance at the surface is predicted when the crystal potential is included.

In Fig. 3 we present experimental STS data obtained at different constant average tunneling currents from the Al(111) surface. Also plotted is the theoretically predicted differential tunneling current as a function of bias voltage for different initial external fields. Oscillations are clearly seen in both the experimental and theoretical data, and their behavior is similar in several impor-

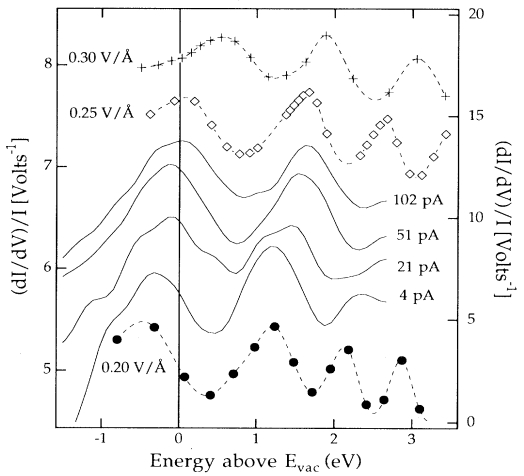

FIG. 3. Experimental (solid curves) and theoretical (symbols) differential conductance curves. Note the similar motion of the oscillations with tunneling current in both sets of curves. For each experimental spectrum, the average tunneling current was held constant at the value indicated. Scattering from the Al lattice was included in the calculations and the assumed initial external field is shown. The dashed curves are cubic spline interpolations between the calculated points. The experimental data refer to the left axis and the theoretical data are scaled to the right axis. All curves, except the lowest experimental and theoretical spectra, are shifted vertically by a constant for clarity.

tant ways. First, the relative peak spacings and intensities seen in the experiment are well reproduced by the calculation and suggest that the experimental data were obtained with an initial external field between 0.20 and 0.25 eV/Å. Second, the peaks and valleys in both the calculated and measured spectra progress to higher bias voltage as the average bias current is increased. This effect is easily understood since for a given voltage, higher tunneling current is obtained by decreasing the tunneling gap resulting in a larger external field that shifts the resonances to higher energy. The most important comparison, however, is for low external field (i.e., low bias current) where one of these resonances occurs below the vacuum level. Comparison of Fig. 3 and Fig. 2 demonstrates that the occurrence of a tunneling resonance below the vacuum level is correlated with a resonance in the surface DOS in this energy range.

From the close correspondence between the IPE data, the STS data, and theoretical modeling we conclude that there exists a crystal-induced electron resonance below E_{vac} on the Al(111) surface. Structure in the IPE spectrum appears to be primarily determined by the surface DOS, although the precise line shape of the spectral feature may be influenced by matrix element effects [13]. Furthermore, we find that the effect of electron scattering from the crystal lattice must not be neglected even in a region far from a band gap when considering the behavior of low energy electrons at simple metal surfaces.

The authors wish to thank R. F. Bell for experimental support. Financial support from the Swedish Natural Science Research Council and the Swedish Board for Technical Developments is gratefully acknowledged.

[a] Present address: Department of Physics, University of Texas at Arlington, Box 19059, Arlington, TX 76019-0059.

[b] To whom correspondence should be addressed.

[1] P. M. Echenique and J. B. Pendry, J. Phys. C **11**, 2065 (1978); E. G. McRae, Rev. Mod. Phys. **51**, 541 (1979).

[2] N. V. Smith, Phys. Rev. B **32**, 3549 (1985); M. Weinert, S. L. Hulbert, and P. D. Johnson, Phys. Rev. Lett. **55**, 2055 (1985); F. J. Himpsel, Comments Condens. Matter Phys. **12**, 199 (1986); J. B. Pendry, C. G. Larsson, and P. M. Echenique, Surf. Sci. **166**, 57 (1986); N. V. Smith, Rep. Prog. Phys. **51**, 1227 (1988); G. D. Kubiak, Surf. Sci. **201**, L475 (1988); P. M. Echenique and J. B. Pendry, Prog. Surf. Sci. **32**, 111 (1989); M. Radny, Surf. Sci. **231**, 43 (1990).

[3] S. A. Lindgren and L. Walldén, Phys. Rev. B **40**, 11 546 (1989).

[4] S. Papadia, M. Persson, and L.-A. Salmi, Phys. Rev. B **41**, 10 237 (1990).

[5] P. Nordlander and J. C. Tully, Surf. Sci. **211/212**, 207 (1989).

[6] R. S. Becker, J. A. Golovchenko, and B. S. Swartzentruber, Phys. Rev. Lett. **55**, 987 (1985).

[7] G. Binnig, K. H. Frank, H. Fuchs, N. Garcia, B. Reihl, H. Rohrer, F. Salvan, and A. R. Williams, Phys. Rev. Lett. **55**, 991 (1985).

[8] J. M. Pitarke, F. Flores, and P. M. Echenique, Surf. Sci. **234**, 1 (1990).

[9] R. Garcia, Phys. Rev. B **42**, 5479 (1990).

[10] R. O. Jones, P. J. Jennings, and O. Jepsen, Phys. Rev. B **29**, 6474 (1984).

[11] A. G. Eguiluz and W. Hanke, Phys. Rev. B **39**, 10 433 (1989); A. G. Eguiluz, M. Heinrichsmeier, A. Fleszar, and W. Hanke, Phys. Rev. Lett. **68**, 1359 (1992).

[12] D. Heskett, K.-H. Frank, E. E. Koch, and H.-J. Freund, Phys. Rev. B **36**, 1276 (1987); D. Heskett, K.-H. Frank, K. Horn, E. E. Koch, H.-J. Freund, A. Baddorf, K.-D. Tsuei, and E. W. Plummer, Phys. Rev. B **37**, 10 387 (1988).

[13] W. L. Schaich and J. T. Lee, Phys. Rev. B **44**, 5973 (1991); W. L. Schaich, Phys. Rev. B **45**, 3744 (1992).

[14] S. Yang, K. Garrison, and R. A. Bartynski, Phys. Rev. B **43**, 2025 (1991).

[15] J. E. Griffith and G. P. Kochanski, Annu. Rev. Mater. Sci. **20**, 219 (1990).

[16] S. Papadia, T. Fondén, and M. Persson (to be published).

[17] F. Schreier and F. Rebentrost, J. Phys. C **20**, 2609 (1987).

[18] P. A. Serena, J. M. Soler, and N. Garcia, Phys. Rev. B **34**, 6767 (1986).

[19] S. P. Singhal and J. Callaway, Phys. Rev. B **16**, 1744 (1977).

[20] N. D. Lang, Phys. Rev. B **34**, 5947 (1986).

[21] G. Paasch and H. Wonn, Phys. Status Solidi (b) **70**, 555 (1975).

[22] K. H. Gundlach, Solid State Electron. **9**, 949 (1966).